Theor Chem Acc (2004) 111:66–77
DOI 10.1007/s00214-003-0521-8

Theoretical Chemistry Accounts

Regular article

Second-order Møller–Plesset second derivatives for the polarizable continuum model: theoretical bases and application to solvent effects in electrophilic bromination of ethylene

Roberto Cammi[1], Benedetta Mennucci[2], Christian Pomelli[2], Chiara Cappelli[2], Stefano Corni[3], Luca Frediani[1], Gary W. Trucks[4], Michael J. Frisch[4]

[1] Dipartimento di Chimica Generale ed Inorganica, Università di Parma, viale delle Scienze, 43100 Parma, Italy
[2] Dipartimento di Chimica e Chimica Industriale, Università di Pisa, via Risorgimento 35, 56126 Pisa, Italy
[3] INFM Center of nanoStructure and bioSystems at Surfaces, Dipartimento di Fisica, Università di Modena e Reggio Emilia, via Campi 213/A, 41100 Modena, Italy
[4] Gaussian Inc., 140 Washington Ave., North Haven, CT 06473, USA

Received: 18 February 2003 / Accepted: 30 April 2003 / Published online: 30 January 2004

Abstract. An analytical theory for the energy second derivatives at second-order Møller–Plesset level for solvated molecules described within the polarizable continuum model is presented. The method, which is based on the differentiation of relaxed density equations for the first derivatives, is firstly presented in its formal aspects and is then applied to the study of the rate-determining step of the electrophilic bromination of ethylene in aqueous solution.

Keywords: Second-order Møller–Plesset – Second derivatives – Continuum solvation – Polarizable continuum model – Electrophilic bromination

1 Introduction

The possibility of computing analytical energy derivatives greatly enhances the ability to accurately characterize chemical systems. Analytical first and second derivatives in fact allow the study of molecular properties and potential-energy surfaces. Owing to the importance of this kind of study great attention has been paid to the formulation of quantum mechanical methods for computing analytical derivatives at different levels of theory [1]. An important extension of such methods is the inclusion of solvent effects; only in this way, in fact, quantitative studies of potential-energy surfaces, chemical reactions and molecular properties involving molecules in condensed phases can be obtained with the same accuracy as calculations for isolated systems.

Contribution to the Jacopo Tomasi Honorary Issue

Correspondence to: B. Mennucci
e-mail: bene@dcci.nnipi.it

This extension was recently begun within solvation models exploiting a continuum description of the solvent [2]. Among the various solvation methods developed so far, the polarizable continuum model (PCM) [3,4] and, in particular, its recent reformulation known as the integral equation formalism (IEF) [5] have been shown to be accurate approaches to compute solvent effects on geometries, energies and properties of molecular solutes [6]. Analytical first and second energy derivatives for the original PCM model within the Hartree–Fock (HF) formalism were introduced in 1994 [7] and then reformulated in the IEF scheme in the late 1990s [8, 9, 10]. Successively, IEF-PCM first derivatives have been extended to post-HF methods such as configuration interaction including single excitations [11], and second-order Møller–Plesset (MP2) [12].

MP2 theory is one of the oldest methods for treating electron correlation and perhaps the most widely used; thus, the extension of continuum solvation models to MP2 methods has been a matter of study for a long time. An ab initio version of the Møller–Plesset perturbation theory within solvation schemes was introduced years ago by Olivares and coworkers [13]. In those papers it was pointed out that electron correlation not only modifies the HF solute charge distribution and the solvent reaction potential, but it is also back-modified by the solvent. To uncouple these combined effects the authors introduced three alternative schemes: the non-iterative "energy-only" scheme, where the solvated HF orbitals are used to calculate MP*n* correlation correction; the density-only scheme where the vacuum MP*n* density matrix is used to evaluate the reaction field; and the iterative scheme, where the correlated electronic density is used to make the reaction field self-consistent.

Successively, it was shown [14] that by applying rigorously the perturbation theory, in which the *n*th order correction to the energy is based on the (*n*-1)th order density, the correct MP2 solute–solvent energy has to be

calculated with the solvent reaction field due to the HF electron density. Following these considerations, the IEF-PCM extension to the MP2 method [12] introduced no iterative procedures involving the electronic density corrected to second-order. This method was thus generalized to the calculation of the analytical energy first derivatives and relaxed MP2 densities within the **Z**-vector technique of Handy and Schaefer [15].

Here we present a further extension of this method to analytical second derivatives. The basis of a large part of the following work is the procedure implemented in the Gaussian package [16] for the evaluation of MP2 second derivatives of isolated systems. This approach is based on the differentiation of the response density equations (Trucks EW, Frisch MJ, Andres JL, Schiegel HB, private communication) and includes several formal and computational advantages, such as the efficient computation of the derivatives of two-electron integrals [17].

The paper is organized as follows: the MP2 energy and MP2 first energy derivatives within the IEF-PCM framework are summarized in Sects. 2 and 3, respectively; The theory of PCM-MP2 second derivatives is presented in Sect. 4; an application to the study of the rate-determining step of the electrophilic addition of bromine to ethylene in aqueous solution is presented in Sect. 5; and, finally, Sect. 6 closes the report with comments and remarks.

2 The PCM-MP2 free energy

At the MP2 level, the free energy of a solvated molecular system can be expressed as

$$\mathscr{G}^{\mathrm{MP2}} = \mathscr{G}^{\mathrm{HF}} + \mathscr{G}^{(2)} \ , \tag{1}$$

where $\mathscr{G}^{\mathrm{HF}}$ is the HF contribution and $\mathscr{G}^{(2)}$ is the MP2 correction.

In an N-electron system described in terms of a single determinant with spin-orbitals expanded over a set of atomic orbitals (AOs) $\{\chi_\mu, \chi_\nu, ...\}$, the HF free energy, $\mathscr{G}^{\mathrm{HF}}$, is written as

$$\begin{aligned}\mathscr{G}^{\mathrm{HF}} = &\sum_{\mu\nu} P^{\mathrm{HF}}_{\mu\nu}(h_{\mu\nu} + j_{\mu\nu}) \\ &+ \frac{1}{2}\sum_{\mu\nu\lambda\sigma} P^{\mathrm{HF}}_{\mu\nu} P^{\mathrm{HF}}_{\lambda\sigma}\left[\langle\mu\lambda||\nu\sigma\rangle + \mathscr{B}_{\mu\nu,\lambda\sigma}\right] + \tilde{V}_{NN} \ ,\end{aligned} \tag{2}$$

where $h_{\mu\nu}$ are the matrix elements, in the AO basis, of the one-electron core operator, $\langle\mu\lambda||\nu\sigma\rangle$ are the antisymmetrized combination of regular two-electron repulsion integrals and $P^{\mathrm{HF}}_{\mu\nu}$ indicates the elements of the HF density matrix

The presence of solvent operators in the effective Hamiltonian is here reflected in the $j_{\mu\nu}$ and $\mathscr{B}_{\mu\nu,\lambda\sigma}$ integrals, which describe the solute–solvent interactions within the PCM model; in particular, the former contain the term due to the nuclei-induced component of the solvent reaction field, while the latter represent the electron-induced counterpart. In the PCM framework the solvent field is described in terms of "apparent" charges placed at the center of small regions (called tesserae) covering the surface of the cavity which contains the molecular solute. In this framework both $j_{\mu\nu}$ and $\mathscr{B}_{\mu\nu,\lambda\sigma}$ are expressed in terms of products of these apparent charges with the electrostatic potential due to the solute nuclear and electronic charge distribution, namely

$$j_{\mu\nu} = -\sum_k V_{\mu\nu}(s_k) q^N(s_k) \tag{3}$$

and

$$\mathscr{B}_{\mu\nu,\lambda\sigma} = -\sum_k V_{\mu\nu}(s_k) q^{\lambda\sigma}(s_k) \ , \tag{4}$$

where

$$q^m(s_k) = \sum_l Q_{kl} V_m(s_l) \text{ with } m = N, \lambda\sigma \tag{5}$$

and V_m contains the solute nuclear ($m = N$) potential and the AO potential integrals ($m = \lambda\sigma$) computed on the cavity tesserae, i.e. at the positions s_k of the apparent charges. All summations are over the total number of tesserae. Details on Eq. (5) defining the apparent charges can be found in Ref.[5]; here we only note that **Q** is a square matrix (the square of the number of tesserae) defined in terms of geometrical parameters of the cavity and the solvent dielectric permittivity. In the last term of Eq. (2), $\tilde{V}_{NN}$, both solute nuclear repulsion and solute–solvent nuclear interaction are included.

The elements $P^{\mathrm{HF}}_{\mu\nu}$ of the HF density matrix are defined as

$$P^{\mathrm{HF}}_{\mu\nu} = \sum_i^N c_{\mu i} c_{\nu i} \ , \tag{6}$$

where $c_{\mu i}$ are the expansion coefficients of molecular spin-orbitals (to simplify the notation, here and in the following we assume real orbitals). They are obtained by solving the corresponding HF equations:

$$\sum_\nu (\tilde{F}_{\mu\nu} - \epsilon_p S_{\mu\nu}) c_{\nu p} = 0 \ , \tag{7}$$

where the elements $\tilde{F}_{\mu\nu}$ of the Fock matrix, namely

$$\tilde{F}_{\mu\nu} = (h_{\mu\nu} + j_{\mu\nu}) + G_{\mu\nu}(\mathbf{P}^{\mathrm{HF}}) + X_{\mu\nu}(\mathbf{P}^{\mathrm{HF}}) \ , \tag{8}$$

contain the solvent effects through the already introduced matrix **j** and through the solvent-equivalent of the in vacuo two-electron matrix **G**; namely we have

$$G_{\mu\nu} = \sum_{\lambda\sigma} P^{\mathrm{HF}}_{\lambda\sigma} \langle\mu\lambda||\nu\sigma\rangle \tag{9}$$

and

$$X_{\mu\nu} = \sum_{\lambda\sigma} P^{\mathrm{HF}}_{\lambda\sigma} \mathscr{B}_{\mu\nu,\lambda\sigma} \ . \tag{10}$$

In Eq. (7) $S_{\mu\nu}$ are the elements of the overlap matrix in the AO basis and ϵ_p is the energy of the pth spin-orbital. In the following the spin-orbitals obtained from Eq. (7) are indicated as $i, j...$ if occupied, $a, b...$ if virtual and $p, q...$ when referring to general molecular orbitals (MOs).

The MP2 contribution to the free energy (Eq. 1) can be written as [13, 14]

$$\mathscr{G}^{(2)} = \frac{1}{4}\sum_{ijab} t_{ij}^{ab}\langle ij||ab\rangle \ , \tag{11}$$

where t_{ij}^{ab} are the double excitation amplitudes

$$t_{ij}^{ab} = \langle ij||ab\rangle/(\epsilon_i + \epsilon_j - \epsilon_a - \epsilon_b) \ . \tag{12}$$

From Eqs. (1), (2), (3), (4), (5), (6), (7), (8), (9), (10), (11) and (12) it follows that the presence of the solvent does not add new terms to the MP2 contribution but implicitly it modifies all the quantities involved (MO coefficients, orbital energies, etc.) with respect to the parallel calculation for the isolated system.

3 MP2-PCM first derivatives

In Ref.[12] we showed that the first derivative of the PCM-MP2 free energy may be written as a contraction of the first derivative of the AO integrals with perturbation-independent MP2 density matrices:

$$\begin{aligned}\mathscr{G}^{\mathrm{MP2},x} = &\sum_{\mu\nu} P_{\mu\nu}^{\mathrm{MP2}}(h_{\mu\nu}^x + j_{\mu\nu}^x) + \sum_{\mu\nu\rho\sigma}\Gamma_{\mu\nu\rho\sigma}^{\mathrm{MP2}}\langle\mu\nu||\rho\sigma\rangle^x \\ &+ \sum_{\mu\nu\lambda\sigma} P_{\mu\nu\lambda\sigma}^{\mathrm{MP2}}\mathscr{B}_{\mu\nu,\lambda\sigma}^x - \sum_{\mu\nu} S_{\mu\nu}^x W_{\mu\nu}^{\mathrm{MP2}} \\ &+ \tilde{V}_{NN}^x \ ,\end{aligned} \tag{13}$$

where the x superscript denotes differentiation of the pertinent integrals with respect to the perturbation parameter x. The details on the calculation of the derivatives, $j_{\mu\nu}^x$ and $\mathscr{B}_{\mu\nu,\lambda\sigma}^x$, of the PCM contributions defined in Eqs.(3), (4) and (5) can be found in Refs. [8, 10].

The one-particle density matrix $\mathbf{P}^{\mathrm{MP2}}$and the energy-weighted density matrix, $\mathbf{W}^{\mathrm{MP2}}$ are given by the sum of the proper HF contribution with a second-order relaxed density matrix correction [18]:

$$P_{\mu\nu}^{\mathrm{MP2}} = P_{\mu\nu}^{\mathrm{HF}} + P_{\mu\nu}^{(2)} \ , \tag{14}$$

$$W_{\mu\nu}^{\mathrm{MP2}} = W_{\mu\nu}^{\mathrm{HF}} + W_{\mu\nu}^{(2)} \ , \tag{15}$$

with $\mathbf{W}^{\mathrm{HF}} = \mathbf{P}^{\mathrm{HF}}\tilde{\mathbf{F}}\mathbf{P}^{\mathrm{HF}}$.

The occupied–occupied and virtual–virtual elements of the relaxed density matrix $\mathbf{P}^{(2)}$ in the MO basis are given by

$$P_{ij}^{(2)} = -\frac{1}{2}\sum_{kab} t_{ik}^{ab} t_{jk}^{ab} \tag{16}$$

and

$$P_{ab}^{(2)} = \frac{1}{2}\sum_{ijc} t_{ij}^{ac} t_{ij}^{bc} \tag{17}$$

and the virtual–occupied block, $P_{ia}^{(2)}$, is obtained as the solution of a single, perturbation-independent, PCM-coupled perturbed HF (CPHF)-like linear equation:

$$\begin{aligned}&\sum_{bj}\left[\langle ij||ab\rangle + \langle aj||ib\rangle + 2\mathscr{B}_{ai,bj}\right]P_{bj}^{(2)} \\ &\quad + (\epsilon_a - \epsilon_i)P_{ai}^{(2)} = \tilde{L}_{ai} \ ,\end{aligned} \tag{18}$$

where $\tilde{L}_{ai}$ are the occupied–virtual elements of the MP2-PCM Lagrangian

$$\begin{aligned}\tilde{L}_{ai} = &\sum_{jk} P_{kj}^{(2)}\left(\langle ki||ja\rangle\right. \\ &\left.+\mathscr{B}_{kj,ai}\right) + \sum_{bc} P_{bc}^{(2)}\left(\langle bi||ca\rangle + \mathscr{B}_{bc,ai}\right) \\ &- \frac{1}{2}\sum_{jkb} t_{kj}^{ab}\langle ib||kj\rangle \\ &+ \frac{1}{2}\sum_{jbc} t_{ij}^{bc}\langle cb||aj\rangle \ .\end{aligned} \tag{19}$$

The elements $P_{\mu\nu}^{(2)}$ are then obtained by back-transformation to the AO basis:

$$P_{\mu\nu}^{(2)} = \sum_{pq} c_{\mu p} c_{\nu q} P_{pq}^{(2)} \ .$$

The relaxed energy-weighted density matrix elements, $W_{pq}^{(2)}$, are given, in the MO basis, by

$$\begin{aligned}W_{ij}^{(2)} = &\frac{1}{2}\sum_{kab} t_{jk}^{ab}\langle ki||ab\rangle - \epsilon_i P_{ij}^{(2)} \\ &- \sum_{pq} P_{pq}^{(2)}\left(\langle ip||jq\rangle + \mathscr{B}_{ij,pq}\right) \ ,\end{aligned} \tag{20}$$

$$W_{ab}^{(2)} = \frac{1}{2}\sum_{ijc} t_{ij}^{bc}\langle ij||ca\rangle - \epsilon_a P_{ab}^{(2)} \tag{21}$$

and

$$W_{ai}^{(2)} = \frac{1}{2}\sum_{jkb} t_{jk}^{ba}\langle jk||ib\rangle - \epsilon_i P_{ai}^{(2)} \tag{22}$$

and the AO elements, $W_{\mu\nu}^{(2)}$, are again obtained by back-transformation of $W_{pq}^{(2)}$.

The semiclassical two-particle density matrix, $P_{\mu\nu\lambda\sigma}^{\mathrm{MP2}}$, is defined as

$$P_{\mu\nu\lambda\sigma}^{\mathrm{MP2}} = \left(\frac{1}{2}P_{\mu\nu}^{\mathrm{HF}} + P_{\mu\nu}^{(2)}\right)P_{\lambda\sigma}^{\mathrm{HF}} \ , \tag{23}$$

while the two-particle density matrix elements, $\Gamma_{\mu\nu\rho\sigma}^{\mathrm{MP2}}$, may be expressed as

$$\Gamma_{\mu\nu\lambda\rho}^{\mathrm{MP2}} = \Gamma_{\mu\nu\lambda\rho}^{\mathrm{S}} + \Gamma_{\mu\nu\lambda\rho}^{\mathrm{NS}} \ , \tag{24}$$

where

$$\Gamma_{\mu\nu\lambda\rho}^{\mathrm{S}} = P_{\mu\nu\lambda\rho}^{\mathrm{MP2}} - P_{\mu\rho\lambda\nu}^{\mathrm{MP2}} \tag{25}$$

and

$$\Gamma_{\mu\nu\lambda\rho}^{\mathrm{NS}} = \sum_{ijab} t_{ij}^{ab} c_{\mu i} c_{\lambda j} c_{\nu a} c_{\rho b} \ . \tag{26}$$

We observe that the structure of Γ^{S} (Eq. 25) is similar to the expression of the HF two-particle density matrix, while Γ^{NS} (Eq. 26) may be viewed as a back-transformation of the excitation amplitude t_{ij}^{ab} from MO to AO basis.

4 MP2-PCM second derivatives

The direct differentiation of the gradient expression (Eq. 13) gives the second derivatives of the PCM-MP2 free energy:

$$\begin{aligned}\mathscr{G}^{\mathrm{MP2},xy} = &\sum_{\mu\nu} P^{\mathrm{MP2}}_{\mu\nu}(h^{xy}_{\mu\nu} + j^{xy}_{\mu\nu}) + \sum_{\mu\nu\rho\sigma} \Gamma^{\mathrm{MP2}}_{\mu\nu\rho\sigma}\langle\mu\nu||\rho\sigma\rangle^{xy} \\ &+ \sum_{\mu\nu\lambda\sigma} P^{\mathrm{MP2}}_{\mu\nu\lambda\sigma}\mathscr{B}^{xy}_{\mu\nu,\lambda\sigma} \\ &- \sum_{\mu\nu} S^{xy}_{\mu\nu} W^{\mathrm{MP2}}_{\mu\nu} + \tilde{V}^{xy}_{NN} + \sum_{\mu\nu} P^{\mathrm{MP2},y}_{\mu\nu}(h^{x}_{\mu\nu} + j^{x}_{\mu\nu}) \\ &+ \sum_{\mu\nu\rho\sigma} \Gamma^{\mathrm{MP2},y}_{\mu\nu\rho\sigma}\langle\mu\nu||\rho\sigma\rangle^{x} \\ &+ \sum_{\mu\nu\lambda\sigma}^{\mathrm{MP2},y} P^{\mathrm{MP2},y}_{\mu\nu\lambda\sigma}\mathscr{B}^{x}_{\mu\nu,\lambda\sigma} - \sum_{\mu\nu} S^{x}_{\mu\nu} W^{\mathrm{MP2},y}_{\mu\nu} \quad , \end{aligned} \tag{27}$$

where the double superscripts xy denote second derivatives of the quantities $A^{xy} = \frac{\partial^2 A}{\partial x \partial y}$.

The second derivatives of the PCM contributions, $j^{xy}_{\mu\nu}$ and $\mathscr{B}^{xy}_{\mu\nu,\lambda\sigma}$, are computed exactly as shown in Ref. [9] for the HF method and thus they will not be considered here. Let us instead focus on the calculation of the MP2-specific terms, namely the first derivatives of the MP2 density matrices, $P^{\mathrm{MP2},y}_{\mu\nu}, P^{\mathrm{MP2},y}_{\mu\nu\rho\sigma}, \Gamma^{\mathrm{MP2},y}_{\mu\nu\rho\sigma}$ and $W^{\mathrm{MP2},y}_{\mu\nu}$ [15, 19, 20].

4.1 One-particle $\mathbf{P}^{\mathrm{MP2},y}$

The first derivatives of the MP2 density matrix, $\mathbf{P}^{\mathrm{MP2},y}$, are obtained as direct differentiation of Eq. (14):

$$P^{\mathrm{MP2},y}_{\mu\nu} = P^{\mathrm{HF},y}_{\mu\nu} + P^{(2),y}_{\mu\nu} \quad , \tag{28}$$

where the derivatives of the HF density, $\mathbf{P}^{\mathrm{HF},y}$, and of the relaxed density contribution, $\mathbf{P}^{(2),y}$, are determined in the following way. The occupied–virtual elements, $P^{\mathrm{HF},y}_{ai}$, in the MO basis are obtained from the solution of the PCM-CPHF system of linear equations

$$\sum_{bj} U^{y}_{bj}(\epsilon_a - \epsilon_i)\tilde{A}_{ai,bj} = \tilde{Q}^{y}_{ai} \quad , \tag{29}$$

where U^{y}_{bj} are the first derivatives of the MO coefficients in the MO basis, and

$$\tilde{A}_{ai,bj} = \delta_{ab,ij} + \frac{\langle ab||ij\rangle + \langle aj||ib\rangle + 2\mathscr{B}_{ai,bj}}{\epsilon_a - \epsilon_i} \quad , \tag{30}$$

and

$$\begin{aligned}\tilde{Q}^{y}_{pq} = &\left(h^{y}_{pq} + j^{y}_{pq}\right) - S^{y}_{pq}\epsilon_q - \sum_{kl} S^{y}_{kl}\left(\langle pl||qk\rangle + \mathscr{B}_{pq,kl}\right) \\ &+ \sum_{\mu\nu\lambda\sigma} c_{\mu p}c_{\nu q}P_{\lambda\sigma}\left(\langle\mu\lambda||\nu\sigma\rangle^{y} + \mathscr{B}^{y}_{\mu\nu,\lambda\sigma}\right) \quad , \end{aligned} \tag{31}$$

with

$$h^{y}_{pq} + j^{y}_{pq} = \sum_{\mu\nu}\left(c_{\mu p}c_{\nu q}(h^{y}_{\mu\nu} + j^{y}_{\mu\nu})\right) \tag{32}$$

and

$$S^{y}_{pq} = \sum_{\mu\nu} c_{\mu p}c_{\nu q}S^{y}_{\mu\nu} \quad . \tag{33}$$

The occupied–occupied elements of the $\mathbf{P}^{\mathrm{HF},y}$ matrix are instead obtained from the first derivatives of the MO orthonormality constraints, and a back-transformation gives $\mathbf{P}^{\mathrm{HF},y}$ in the AO basis:

$$P^{\mathrm{HF},y}_{\mu\nu} = \sum_{pq}\left(c^{y}_{\mu p}P^{\mathrm{HF}}_{pq}c_{\nu q} + c_{\mu p}P^{\mathrm{HF},y}_{pq}c_{\nu q} + c_{\mu p}P^{\mathrm{HF}}_{pq}c^{y}_{\nu q}\right) \tag{34}$$

with

$$c^{y}_{\sigma i} = \sum_{p} U^{y}_{pi}c_{\sigma p} \quad .$$

The occupied–occupied and virtual–virtual blocks of $P^{(2),y}_{pq}$ in the MO basis, are instead given by

$$P^{(2),y}_{ij} = -\frac{1}{2}\sum_{kab}\left(\tau^{ab}_{ik}t^{ab}_{jk} + t^{ab}_{ik}\tau^{ab}_{jk}\right) \tag{35}$$

and

$$P^{(2),y}_{ab} = \frac{1}{2}\sum_{ijc}\left(\tau^{ab}_{ij}t^{bc}_{ij} + t^{ab}_{ij}\tau^{bc}_{ij}\right) \quad , \tag{36}$$

where $\left\{\tau^{ab}_{ij}\right\}$ are the derivatives of the double-excitation amplitudes:

$$\begin{aligned}\tau^{ab}_{ij} = &\frac{\partial t^{ab}_{ij}}{\partial y} \\ = &\frac{<ij||ab>^{y} + \sum_d\left(f^{y}_{bd}t^{ad}_{ij} + f^{y}_{ad}t^{db}_{ij}\right) - \sum_k\left(f^{y}_{kj}t^{ab}_{ik} + f^{y}_{ki}t^{ab}_{kj}\right)}{(\epsilon_i + \epsilon_j - \epsilon_a - \epsilon_b)} , \end{aligned} \tag{37}$$

with

$$\begin{aligned}\langle pq||rs\rangle^{y} = &\sum_{\mu\nu\lambda\sigma}(c_{\sigma r}c_{\lambda s} - c_{\sigma s}c_{\lambda r})c_{\mu p}c_{\nu q}\langle\mu\nu|\lambda\sigma\rangle^{y} \\ &+ \sum_{i}\Big(\langle tq||rs\rangle U^{y}_{tp} + \langle pt||rs\rangle U^{y}_{tq} + \langle pq||ts\rangle U^{y}_{tr} \\ &+ \langle pq||rt\rangle U^{y}_{ts}\Big) \end{aligned} \tag{38}$$

and

$$\begin{aligned}f^{y}_{pq} = &h^{y}_{pq} + S^{y}_{pq}\xi_{pq} - \sum_{kl} S^{y}_{kl}\langle pl||qk\rangle \\ &+ \sum_{\mu\nu\lambda\sigma} c_{\mu p}c_{\nu q}P_{\lambda\rho}(\langle\mu\nu||\lambda\sigma\rangle^{y} + \mathscr{B}^{y}_{\mu\nu,\lambda\sigma}) \\ &+ \sum_{qm} U^{y}_{qm}\left(\langle pm||qq\rangle + \langle pq||qm\rangle + 2\mathscr{B}_{pq,mq}\right) \quad , \end{aligned} \tag{39}$$

where

$$\xi_{pq} = \begin{cases} \frac{1}{2}(\epsilon_p + \epsilon_q) & p,q \in \text{ occupied or } p,q \in \text{ virtual} \\ \epsilon_q & \text{otherwise} \end{cases}$$

The occupied–virtual block $P^{(2),y}_{ai}$ is obtained by solving the linear system of equations

$$\sum_{jb}\left(\langle ij||ab\rangle + \langle aj||ib\rangle + 2\mathscr{B}_{ai,bj}\right)P^{(2),y}_{bj} + (\epsilon_a - \epsilon_i)P^{(2),y}_{ai} = \hat{L}^{(2)y}_{ai} \quad , \tag{40}$$

where

$$\hat{L}^{(2)y}_{ai} = \tilde{L}^{(2),y}_{ai} + \sum_{jb}\left(\langle ij||ab\rangle^y + \langle ib||ja\rangle^y + 2\mathscr{B}^y_{ai,bj}\right)P^{(2),y}_{bj} - f^y_{ab}P^{(2)}_{bi} + f^y_{ji}P^{(2)}_{aj} \quad , \tag{41}$$

with the derivative Lagrangian $\tilde{L}^{(2),y}_{ai}$ given by

$$\begin{aligned}\tilde{L}^{(2),y}_{ai} = &\sum_{jk}P^{(2),y}_{kj}\left(\langle ki||ja\rangle + \mathscr{B}_{kj,ai}\right) + \sum_{jk}P^{(2),y}_{kj}\left(\langle ki||ja\rangle + \mathscr{B}_{kj,ai}\right) \\ &+ \sum_{bc}P^{(2)}_{bc}\left(\langle bi||ca\rangle^y + \mathscr{B}^y_{bc,ai}\right) + \sum_{bc}P^{(2)}_{bc}\left(\langle bi||ca\rangle^y + \mathscr{B}^y_{bc,ai}\right) \\ &- \frac{1}{2}\sum_{jkb}\tau^{ab}_{kj}\langle ib||kj\rangle - \frac{1}{2}\sum_{jkb}t^{ab}_{kj}\langle ib||kj\rangle^y \\ &+ \frac{1}{2}\sum_{jbc}\tau^{bc}_{ij}\langle cb||aj\rangle + \frac{1}{2}\sum_{jbc}t^{bc}_{ij}\langle cb||aj\rangle^y\end{aligned} \tag{42}$$

and

$$\begin{aligned}\mathscr{B}^y_{pq,rs} = &\sum_{\mu\nu\lambda\sigma}c_{\sigma r}c_{\lambda s}c_{\mu p}c_{\nu q}\mathscr{B}^y_{\mu\nu\lambda\sigma} \\ &+ \sum_i\left(\mathscr{B}_{trqs}U^y_{tp} + \mathscr{B}_{prts}U^y_{tq} + \mathscr{B}_{ptqs}U^y_{tr} + \mathscr{B}_{prqt}U^y_{ts}\right) \quad .\end{aligned} \tag{43}$$

The elements of $\mathbf{P}^{(2),y}$ in the MO basis are then back-transformed to the required AO basis representation as

$$P^{(2),y}_{\mu\nu} = \sum_{pq}\left(c^y_{\mu p}P^{(2)}_{pq}c_{\nu q} + c_{\mu p}P^{(2),y}_{pq}c_{\nu q} + c_{\mu p}P^{(2)}_{pq}c^y_{\nu q}\right) \quad . \tag{44}$$

4.2 Two-particle $\mathbf{P}^{\mathrm{MP2},y}$

The first derivatives of the two-particle MP2 density matrix $\mathbf{P}^{\mathrm{MP2},y}$ is obtained as differentiation of the constituted (Eq. 23):

$$P^{\mathrm{MP2},y}_{\mu\nu\lambda\sigma} = \left(\frac{1}{2}P^{\mathrm{HF},y}_{\mu\nu} + P^{(2),y}_{\mu\nu}\right)P^{\mathrm{HF}}_{\lambda\sigma} + \left(\frac{1}{2}P^{\mathrm{HF}}_{\mu\nu} + P^{(2)}_{\mu\nu}\right)P^{\mathrm{HF},y}_{\lambda\sigma} \tag{45}$$

4.3 $\mathbf{W}^{\mathrm{MP2},y}$

The first derivative of the energy-weighted MP2 density matrix $\mathbf{W}^{\mathrm{MP2},y}$, is obtained by differentiating Eq. (15)

$$W^{\mathrm{MP2},y}_{\mu\nu} = W^{\mathrm{HF},y}_{\mu\nu} + W^{(2),y}_{\mu\nu} \quad . \tag{46}$$

The HF matrix contribution, $\mathbf{W}^{\mathrm{HF},y}$, is given by

$$\mathbf{W}^{\mathrm{HF},y} = \mathbf{P}^{\mathrm{HF},y}\tilde{\mathbf{F}}\mathbf{P}^{\mathrm{HF}} + \mathbf{P}^{\mathrm{HF}}\tilde{\mathbf{F}}^y\mathbf{P}^{\mathrm{HF}} + \mathbf{P}^{\mathrm{HF}}\tilde{\mathbf{F}}\mathbf{P}^{\mathrm{HF},y} \quad . \tag{47}$$

The elements of the differentiated relaxed correction, $W^{(2),y}_{pq}$, are given, in the MO basis, by

$$\begin{aligned}W^{(2),y}_{ij} = &\frac{1}{2}\sum_{kab}\tau^{ab}_{jk}\langle ki||ab\rangle + \frac{1}{2}\sum_{kab}t^{ab}_{jk}\langle ki||ab\rangle^y \\ &- \sum_k f^y_{ik}P^{(2),y}_{kj} - \epsilon_i P^{(2),y}_{ij} \\ &- \sum_{pq}P^{(2)}_{pq}\left[\langle ip||jq\rangle^y + \mathscr{B}^y_{ij,pq}\right] \quad ,\end{aligned} \tag{48}$$

$$\begin{aligned}W^{(2),y}_{ab} = &\frac{1}{2}\sum_{ijc}\tau^{bc}_{ij}\langle ij||ca\rangle + \frac{1}{2}\sum_{ijc}t^{bc}_{ij}\langle ij||ca\rangle^y \\ &- \sum_c f^y_{ac}P^{(2),y}_{cb} - \epsilon_a P^{(2),y}_{ab}\end{aligned} \tag{49}$$

and

$$\begin{aligned}W^{(2),y}_{ai} = &\frac{1}{2}\sum_{jkb}\tau^{ba}_{jk}\langle jk||ib\rangle + \frac{1}{2}\sum_{jkb}t^{ba}_{jk}\langle jk||ib\rangle^y \\ &- \sum_k f^y_{ik}P^{(2),y}_{ak} - \epsilon_i P^{(2),y}_{ai}\end{aligned} \tag{50}$$

and a back-transformation gives the density matrix derivatives, $\mathbf{W}^{\mathrm{HF},y}$ and $\mathbf{W}^{(2),y}$ in the AO basis representation

$$W^{X,y}_{\mu\nu} = \sum_{pq}\left(c^y_{\mu p}W^X_{pq}c_{\nu q} + c_{\mu p}W^{X,y}_{pq}c_{\nu q} + c_{\mu p}W^X_{pq}c^y_{\nu q}\right), \quad X = \mathrm{HF}, (2) \quad . \tag{51}$$

4.4 $\mathbf{\Gamma}^{\mathrm{MP2},y}$

Direct differentiation of Eq. (24) gives the derivatives of the two-particle density matrix derivative, $\Gamma^{\mathrm{MP2},y}_{\mu\nu\lambda\sigma}$, as

$$\Gamma^{\mathrm{MP2},y}_{\mu\nu\lambda\rho} = \Gamma^{\mathrm{S},y}_{\mu\nu\lambda\rho} + \Gamma^{\mathrm{NS},y}_{\mu\nu\lambda\rho} \quad , \tag{52}$$

with

$$\begin{aligned}\Gamma^{\mathrm{S},y}_{\mu\nu\lambda\rho} = &\frac{1}{2}(P^{\mathrm{HF},y}_{\mu\nu} + 2P^{(2),y}_{\mu\nu})P^{\mathrm{HF}}_{\lambda\rho} + \frac{1}{2}(P^{\mathrm{HF}}_{\mu\nu} + 2P^{(2)}_{\mu\nu})P^{\mathrm{HF},y}_{\lambda\rho} \\ &- \frac{1}{2}(P^{\mathrm{HF},y}_{\mu\rho} + 2P^{(2),y}_{\mu\rho})P^{\mathrm{HF}}_{\lambda\nu} - \frac{1}{2}(P^{\mathrm{HF}}_{\mu\rho} + 2P^{(2)}_{\mu\rho})P^{\mathrm{HF},y}_{\lambda\nu}\end{aligned} \tag{53}$$

and

$$\begin{aligned}\Gamma^{\mathrm{NS},y}_{\mu\nu\lambda\rho} = &\sum_{ijab}\tau^{ab}_{ij}c_{\mu i}c_{\lambda j}c_{\nu a}c_{\rho b} + \sum_{ijab}t^{ab}_{ij}C^y_{\mu i}c_{\lambda j}c_{\nu a}c_{\rho b} \\ &+ \sum_{ijab}t^{ab}_{ij}c_{\mu i}c^y_{\lambda j}c_{\nu a}c_{\rho b} + \sum_{ijab}t^{ab}_{ij}c_{\mu i}c_{\lambda j}c^y_{\nu a}c_{\rho b} \\ &+ \sum_{ijab}t^{ab}_{ij}c_{\mu i}c_{\lambda j}c_{\nu a}c^y_{\rho b} \quad .\end{aligned} \tag{54}$$

We conclude this section by observing that the evaluation of the second derivatives of the PCM-MP2 free

energy requires the solution of two sets of CPHF-like equations, one for the evaluation of the derivatives of the MO coefficients and the other for the calculation of the derivatives of the relaxed density matrix. This leads to an increase of the computational complexity with respect to the corresponding calculation performed at the HF/density functional theory level, which, conversely, requires the solution of only one PCM-CPHF equation.

However, by introducing a reverse form of the interchange theorem, it is possible to avoid the explicit evaluation of the occupied–virtual elements of the derivative of the relaxed density matrix, $P_{ai}^{(2),y}$, and the necessity to solve the corresponding set of equations. In fact, looking at the second derivative Eq. (27) it is not difficult to note that in the MO basis the contraction involving the elements $P_{ai}^{(2),y}$ may be written as

$$\sum_{ai} P_{ai}^{(2),y}\Big[h_{ai}^{x} + j_{ai}^{x} - \sum_{jk}(\langle ja\|ki\rangle + \mathscr{B}_{jk,ai})S_{jk}^{x} - \epsilon_i S_{ai}^{x} - G_{ai}^{x} - X_{ai}^{x}\Big] = \sum_{ai} P_{ai}^{(2),y}\tilde{Q}_{ai}^{x} \quad . \tag{55}$$

Further, by rearranging Eq. (40) as

$$\sum_{bj} P_{bj}^{(2),y}(\epsilon_b - \epsilon_j)\tilde{A}_{bj,ai} = \hat{L}_{ai}^{(2),y} \tag{56}$$

we obtain

$$P_{ai}^{(2),y} = \sum_{bj} \frac{\hat{L}_{bj}^{(2),y}}{\epsilon_b - \epsilon_i}\left(\tilde{A}^{-1}\right)_{bj,ai} \quad . \tag{57}$$

Then, by introducing Eq. (57) into Eq. (55) it follows that

$$\sum_{ai} P_{ai}^{(2),y}\tilde{Q}_{ai}^{x} = \sum_{ai}\sum_{bj} \frac{\hat{L}_{bj}^{(2),y}}{\epsilon_b - \epsilon_i}\left(\tilde{A}^{-1}\right)_{bj,ai}\tilde{Q}_{ai}^{x} = \sum_{bj} \hat{L}_{bj}^{(2),y}U_{bj}^{x} \quad . \tag{58}$$

Therefore the contraction involving the relaxed density derivative, $P_{ai}^{(2),y}$, may be expressed as the product of the total derivative Lagrangian with the CPHF coefficients. As this provides the complete contribution from $P_{ai}^{(2),y}$, all second-derivative terms involving the derivative density are limited to the occupied–occupied and virtual–virtual blocks. This is in fact the **Z**-vector method of Handy and Schaefer applied in reverse.

The reverse interchange for second derivatives was originally developed by Tracks et al. (Trucks EW, Frisch MJ, Andres JL, Schlegel HB, Private communication); here we have shown how the solvent reaction terms modify the general procedure, and how these changes affect the derivatives of energies and densities.

5 Application to chemical reactions in solution: the addition of bromine to ethylene

The study of a reaction mechanism may be done by performing a well-determined sequence of computational steps that can be defined as the canonical approach to the study of chemical reactions. At first, one has to determine the geometry of reactants and products, then that of locally stable intermediates, especially those acting as precursors of the true reaction process, and finally that of the transition state (TS) or TSs and of the reaction intermediates, if any. As all these points are stationary points on the potential-energy surface, the calculation of first and second derivatives of the energy with respect to nuclear coordinates becomes the fundamental tool in their localization and characterization.

The following step in the canonical procedure is the determination of the reaction path (RP) or of the corresponding curvilinear coordinate, often called reaction coordinate, or more specifically intrinsic reaction coordinate (IRC) [21, 22].

Once the energy profile of the IRC, and the corresponding changes in the internal geometry of the system have been determined, the first goal in the canonical description of the mechanism is reached. A possible extension, and at the same time a completion, is the interpretation of what has been computationally found. Such interpretation is usually based on clear and simple physical and chemical concepts which are represented by appropriate theoretical and computational tools such as, for example, the shape of localized charge distributions or other suitable indices.

The further steps in the study of reaction mechanisms go beyond the canonical procedure, and in the general sense they begin to consider dynamic aspects of the reaction still in the framework of the concept of the RP defined earlier [23, 24].

This basic theoretical and computational scheme was originally defined for systems reacting in the gas phase but its extension to solvated systems is feasible. One of the most systematic contributions to the theoretical reformulation of the canonical approach for solvated systems has been given by the works of Tomasi [25]. Following his analysis some well-defined aspects can be identified [2, 26]. Not only all the steps of the canonical procedure have to be redefined so to account for solvation effects on structures, energies and properties of the reacting systems, but also solvent-specific aspects have to be introduced. First, new coordinates, generally indicated as solvent coordinates, have to be added to account for the effects of the retarding forces (frictions) induced by the solvent molecules not in equilibrium with the reacting system. Second, the solvent molecules have an intrinsic thermal motion which may induce local fluctuations in their distribution around the solute, and thus affect the reaction rate or the apparent reaction barrier. Third, one or more solvent molecules can be directly involved in the reaction, for example, by exerting a catalytic role.

Here we present an application of some of these concepts to the study of the rate-determining step of the electrophilic addition of bromine to ethylene in the gas phase and in water solution. As the subject of this paper is the theoretical and computational method defining the analytical MP2 second derivatives for solvated systems, attention will be mainly focussed on those aspects of the canonical approach to the study of reactions that more

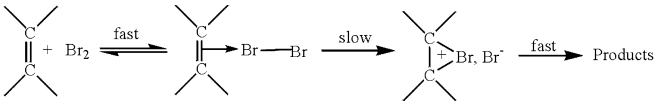

directly involve the calculation of these derivatives (both with respect to nuclear coordinates and external electric fields).

The addition of halogens to carbon-carbon double bonds is interpreted as a stepwise addition which is initiated by a species containing a positively polarized halogen: in the present case the bromine molecule which becomes polarized in close proximity to the π-electron cloud of ethylene. The initial step results in the formation of a "T-shaped" charge–transfer intermolecular complex (CTC) [27] which has been identified both theoretically [28, 29, 30] and experimentally [31, 32] in the gas phase. Such a complex can thus evolve towards the heterolytic breaking of the Br–Br σ bond and to the formation of a cyclic three-membered bromonium ion intermediate.

It is well known experimentally [33] and theoretically [34] that the formation of the bromonium ion from an ethylenic bond and a bromine molecule is impossible in the gas phase. The same reaction becomes possible in solution [35] in which the rate-determining step is that following the fast and reversible formation of the bromine–olefin CTC and leading to the ionic intermediate by unimolecular dissociation of the CTC. The existence of such intermediates and their occurrence in bromination are supported by spectroscopic observations and kinetic measurements which show high sensitivities to solvent and substituent change. The dissociation of the olefin–bromine CTC is thought to be assisted by the solvent in protic media and by a second bromine in nonprotic media [38].

Theoretical studies of the thermodynamic stability of the bromonium intermediate in solution [36] and of the effect of the dielectric constant of the solvent on the reaction mechanism [37] have been made. Here, we present a detailed MP2 study on the RP leading from the CTC to the TS for the addition of Br_2 to ethylene both in the gas phase and in water. Such a study involves the calculation of the structures, the energies and the vibrational frequencies of the CTC and the TS and the analysis of the RP in terms of different reactivity indices. The effects of solvation are introduced through the IEF-PCM continuum: for all systems four interlocked spheres (centered on the C and Br atoms) and the dielectric constant of water (78.54) were used to describe the solute cavity and the solvent dielectric response, respectively.

It is known that a proper description of the complexes between bromine and olefins requires a high level of theory. In fact, the interactions in these complexes are of dispersive and charge-transfer nature and thus a correlated method and a basis set with polarization and diffuse functions are indispensable. There is a systematic work [30] that shows that the widely used density functional methods do not give an adequate description of such kinds of systems; the B3LYP functional is the one that gives better results, but for an accurate description at least a MP2 calculation is required.

With regard to the choice of a proper basis set, polarization and diffuse functions are surely to be included, but the presence of the bromine atoms also requires the use of effective core potentials (ECPs). Among the basis sets available in the Gaussian package, the CEP-121G basis set [38] was chosen as it includes a relativisitic ECP for Br. This set was augmented by diffuse and polarization functions; namely three d and one f function were added on Br, one p and one d on C, and one p function on H. In the following the resulting basis set is indicated as CEP-121G(aug). The reliability of this effective core basis set was checked by comparison with full-electron calculations using different extended basis sets.

5.1 Structures of the CTC and the TS and the RP

At the MP2/CEP-121G(aug) level the structures of the CTC and the TS have C_{2v} symmetry both in the gas phase and in water; the optimized structures with an indication of the main geometrical parameters are reported in Fig. 1.

In previous studies a C_s symmetry was also found for the gas-phase TS at the HF level of theory [34,37]. however, a later complete-active-space-self-consistent-field study [39] on the potential-energy surface for the electrophilic addition of chlorine to ethylene in the gas phase and in aqueous solution showed the validity of the symmetric C_{2v}.

The characterization of both structures was confirmed by a frequency analysis. In particular, it was verified that the TS structures present the characteristic imaginary frequency corresponding to the transition vector; this is illustrated in Fig. 2 for both gas-phase and water TSs.

The results of Figs. 1 and 2 indicate that, while the CTC is not very different in the gas phase and in water

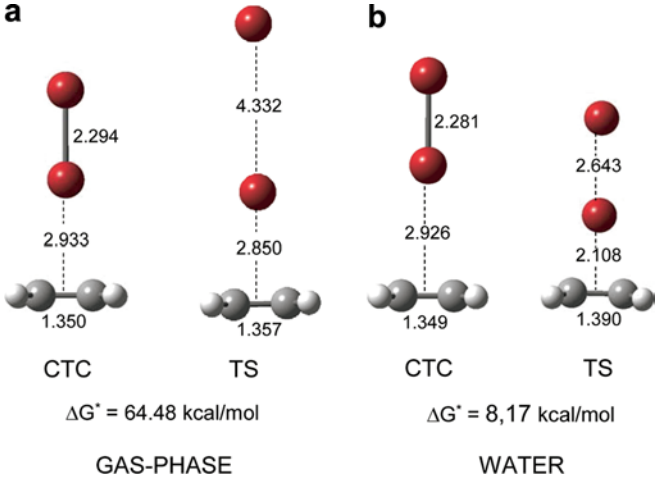

Fig. 1. Second-order Møllar–plesset (*MP2*)/CEP-121(aug) structure for the charge-transfer complex (*CTC*) and the transition state (*TS*) in the gas phase and in water. The distances between bromine atoms, and between the CC bond midpoint and the nearest bromine are shown (Å) together with the activation free energies

and thus for this system the solvent effects are not very important, the structure of the TS is largely affected by the presence of the solvent. As expected, the solvated TS has an earlier character with a Br–Br bond much shorter than in the gas phase.

The localization and characterization of the CTC and TS structures also allow the calculation of activation barriers. As in previous studies [34], our MP2 calculation for the isolated system gives an activation barrier of more than 60 kcal mol^{-1} as shown in Fig. 1. As expected, the effects of solvation lower the barrier, making the formation of the bromonium ion intermediate possible. This is expected as the TS is rather polar and it has a larger solvation energy. After including entropy and zero-point effects, the computed IEF-PCM barrier becomes 8.17 kcal mol^{-1}; this value agrees well with the estimate of less than 10 kcal mol^{-1} obtained from the bromination rate constant observed in water [40].

Before going further in the canonical procedure described previously, it is useful to have a direct estimate of correlation effects. We thus recalculated the CTC and TS structures in water at the HF level with the same basis set used for the MP2 calculations. The HF geometrical parameters and the relative activation barrier are reported in Table 1.

The comparison of the results of Fig. 1 and Table 1 shows that correlation effects are different in the CTC and in the TS, and that they differently affect the solvent reaction fields in the two structures. Correlation effects are in fact much larger in the TS: the HF structure presents a longer Br–Br bond and a shorter Br–CC midpoint distance with respect to MP2; this seems to indicate an earlier character for the MP2 TS with respect to the uncorrelated HF analog. This larger sensitivity of the solvated TS structure to the electronic correlation can be explained with the larger magnitude of the reaction field at the TS. This correlation effect is also reflected in the value of the activation barrier, which lowers by about 1.7 kcal mol^{-1} on passing from the HF to the MP2 level.

As requested by the canonical procedure, once the main stationary points have been localized and characterized, the following step is the determination of the RP; this was limited here to the CTC-to-TS branch and it was obtained by using the method of Schlegel and co workers [22].

As an example, in Fig. 3 we report the illustration of the RP obtained in water; a similar but much more extended plot (both in the values of the reaction coordinate and the energy) was obtained for the gas phase. In the graph the TS corresponds to the zero of the reaction coordinate, and this assumes negative values going back toward the CTC.

The comparison of RPs calculated for the gas phase and for water shows that the presence of the solvent not only changes the barrier height but it also significantly affects the nature of the reaction coordinate. This can be better shown in terms of the variation of the distances R_{CC}, R_{BrBr} and R_{BrCC} along the RP in the gas phase and in water as illustrated in Figs. 4 and 5.

As can be seen from Fig. 4, in the gas phase the functions representing the distance between the incoming bromine and the CC midpoint (R_{BrCC}) and between the two carbons (R_{CC}) are not monotonic but they present a shallow minimum and a parallel maximum. This seems to indicate that the gas-phase reaction coordinate is more complex and that it does not exactly coincide with the Br–CC distance. In water, in contrast, all three distances show monotonic behavior as expected.

The RP was also analyzed in the scheme of the RP Hamiltonian (RPH) method [23]. This characterizes the reaction in terms of motion along the RP and vibrational motion orthogonal to this path. From the analysis of the terms of the RPH, one can obtain insight into qualitative features of the reaction mechanism and reaction dynamics.

In this study the application of the RPH is limited to static aspects; here we in fact analyzed the two modes

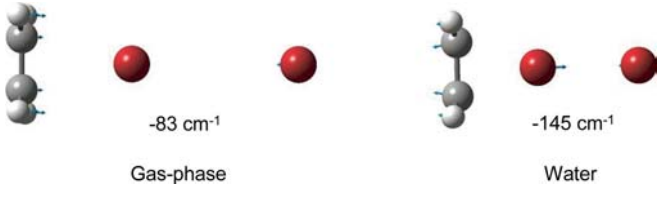

Fig. 2. Transition vector and relative frequency for the TS in the gas phase and in water

Table 1. Hartree–Fock/CEP-121G(aug) distances (Å) for the charge-transfer-complex (CTC) and the transition state (TS) and the activation energy, ΔG^* (kcal mol^{-1})

	CTC	TS
R_{BrBr}	2.271	3.452
R_{CC}	1.329	1.439
R_{BrCC}	3.715	1.940
ΔG^*	9.79	

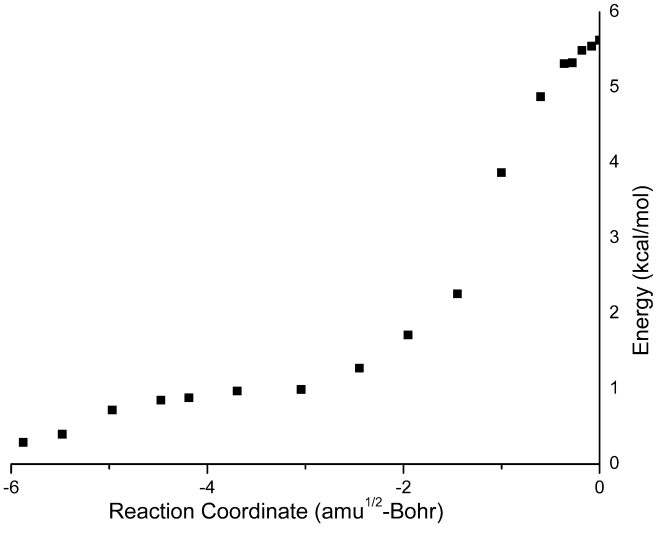

Fig. 3. TS-to-CTC reaction path computed at the MP2 level for the system in water

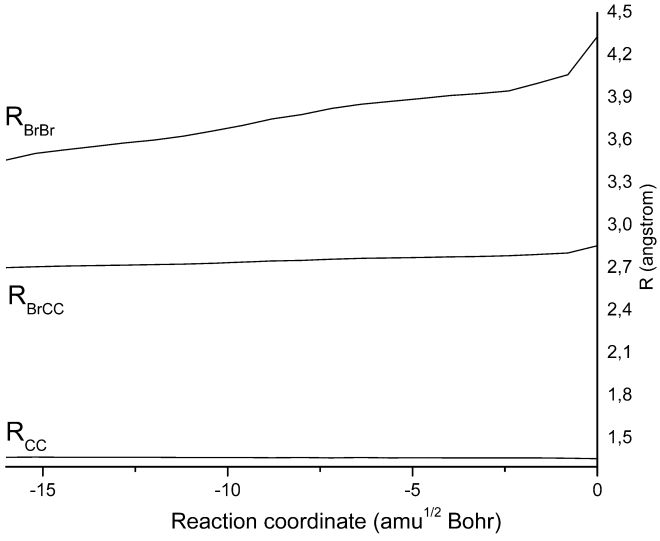

Fig. 4. R_{CC}, R_{BrBr} and R_{BrCC} distances (Å) along the reaction path for Br_2 addition to C_2H_2 in the gas phase

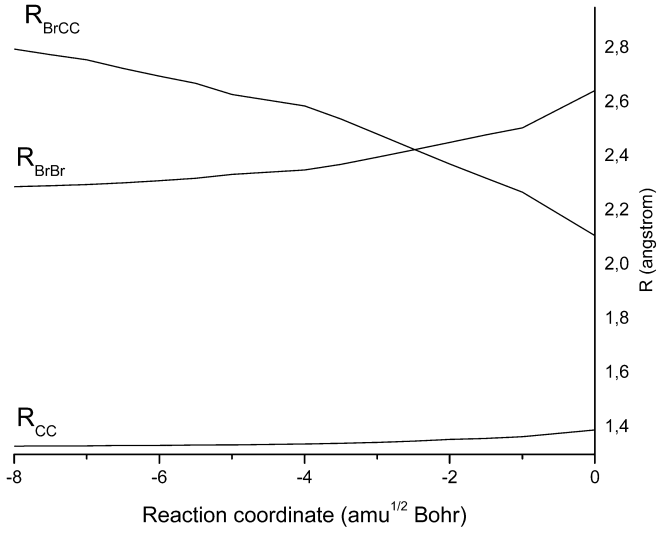

Fig. 5. R_{CC}, R_{BrBr} and R_{BrCC} distances (Å) along the reaction path for Br_2 addition to C_2H_2 in water

which are more strongly coupled to the reaction coordinate for the system in water. The second derivative matrix was calculated at each point on the RP, projected to remove motion along the RP as well as overall translational and rotational motion, and finally diagonalized to give the harmonic frequencies. The variation of these frequencies (for the two selected modes) along the RP is shown in Fig. 6.

Looking at the normal modes corresponding to the two selected frequencies, we find that they correspond to the 1383 and 1754-cm^{-1} modes of the TS; they are illustrated in Fig. 7. As can be seen from Fig. 7 the lower-frequency mode involves a stretching along the CC bond, while the second is a bending of the CH moieties coupled with a weak CC stretching. Moving back from the TS to the CTC both frequencies increase; in particular the lower-frequency mode varies from

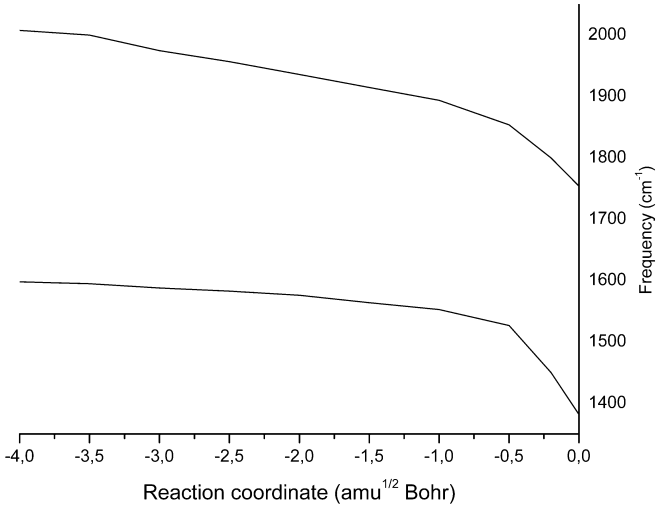

Fig. 6. Projected vibrational frequencies (cm^{-1}) with respect to the reaction coordinate for the addition of Br_2 to C_2H_2 in water

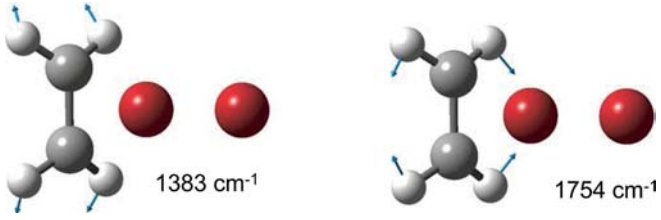

Fig. 7. Normal modes for the TS in water which present the largest coupling with the reaction coordinate

stretching to bending, while the higher-frequency mode increases the CC stretching component.

5.2 Analysis of properties along the RP

To further investigate solvation effects, we performed along the RPs analyses of the wavefunction by using the natural bond orbital (NBO) method [41] and of the polarizability tensor.

We report the NBO natural atomic charge (nuclear charge minus summed natural populations of natural AOs on the atom) on C and Br atoms, in Table 2 whereas in Figs. 8 and 9 we illustrate the same natural charges as a function of the reaction coordinate (in the gas-phase graph we extrapolated the values of the charges beyond the computed RP to illustrate the crossing of Br1 and Br2 at the limit corresponding to the CTC).

The main result of the NBO analysis is the large difference in the natural charge of bromine atoms in the gas phase and in water. These charges clearly indicate that the nature of the TS is completely different in the isolated and in the solvated system as already indicated by the very different geometries (see Fig. 1). In particular, in the gas phase the partially negative charge on the incoming bromine (Br1) indicates that in this case there are no electrostatic interactions with the ethylene moiety

Table 2. Natural charges on C and Br atoms in the CTC and the TS in the gas phase and in water. *Br*1 refers to the bromine atom closer to the CC bond. Charges are in atomic units

	Gas		Water	
	CTC	TS	CTC	TS
C	−0.3106	−0.2392	−0.3056	−0.2281
Br1	+0.0080	−0.3855	+0.0069	+0.2519
Br2	−0.0513	+0.1857	−0.0572	−0.6067

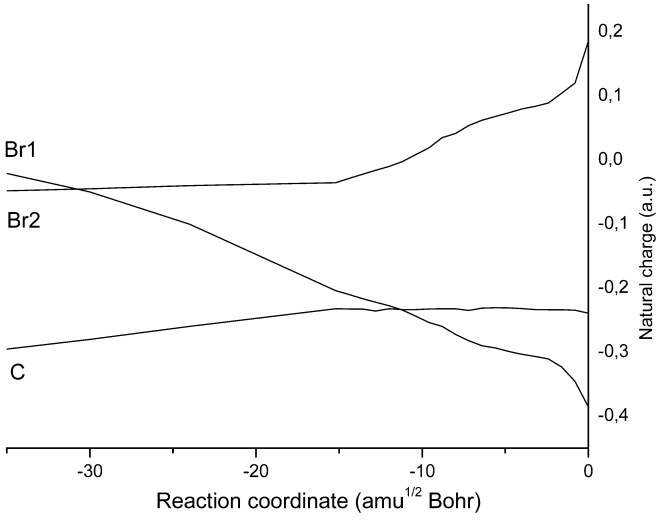

Fig. 8. Natural charges on C and Br atoms as a function of the reaction coordinate for Br_2 addition to C_2H_2 in the gas phase

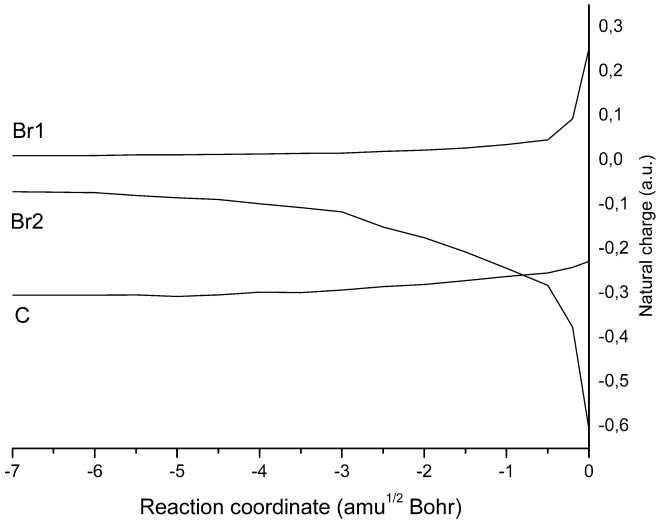

Fig. 9. Natural charges on C and Br atoms as a function of the reaction coordinate for Br_2 addition to C_2H_2 in water

and thus the activated complex is mainly of dispersive character (this is also reflected in the long R_{BrCC} distance in the TS). Such a description is completely reversed in water, where the Br–CC interaction presents clear and strong electrostatic character and the two bromines

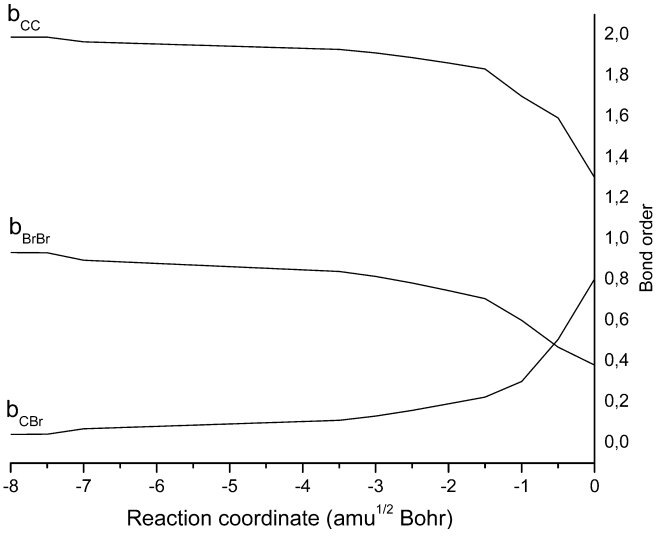

Fig. 10. CC, CBr, and BrBr bond orders as a function of the reaction coordinate for Br_2 addition to C_2H_2 in water

present the expected separation of charge in the region around the TS. To confirm this analysis we also note that the dipole of the TS goes from 1.10 D in the gas phase to 12.74 D in water (the CTC presents a dipole moment of about 1.5 D both in the gas phase and in water).

A more "chemical" analysis of the effect of the solvent on the nature of the TS can be obtained in terms of the variation in the bonding pattern along the RP. This variation is quantified by the CC, BrBr and CBr bond order values with respect to the reaction coordinate as reported in Fig. 10.

All the calculated bond orders are seen to vary with the reaction coordinate in a continuous and physically reasonable manner. In fact, consistent with the expected picture, moving from the CTC to the TS, the C–C bond order smoothly decreases from double-bond ($b_{CC} \sim 2$) to single-b and ($b_{CC} \sim 1$) character. The CBr bond order correspondingly increases from non bonded ($b_{CBr} \sim 0$) to single-bond character, while the B_rB_r bond order simultaneously decreases from single-bonded character to non bonded. These bond order switches are all approximately "70% complete" at the TS ($b_{CC} = 1.3$ instead of 1, $b_{CBr} = 0.8$ instead of 1 and $b_{BrBr} = 0.38$ instead of 0).

An alternative analysis to natural charges and bond orders but still strictly dependent on the variation in the charge distribution along the RP is that in terms of the polarizability. There is analytical and numerical evidence [42] showing that the polarizability has a very close link with theoretical indices developed to measure the sensitivity of the electron density to structural perturbations and responses to the changes in external conditions. We can thus predict that the polarizability can reflect the chemical reactivity of a system.

We report the three diagonal components of the polarizability tensor and the isotropic value with respect to the reaction coordinate for both gas-phase and solvated systems Figs. 11 and 12; we recall that the bromine

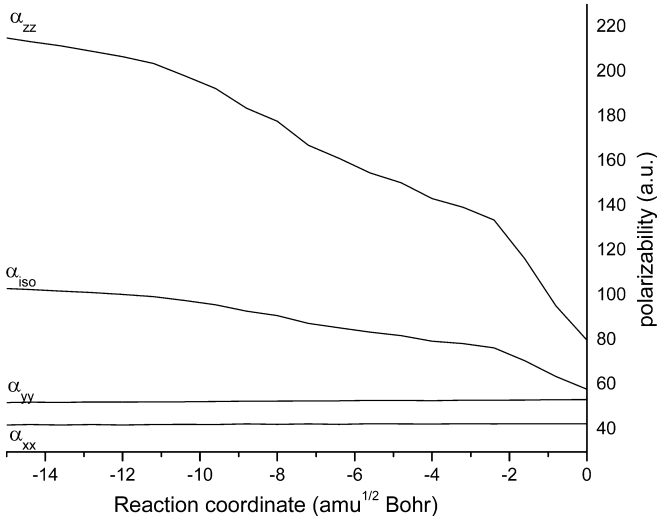

Fig. 11. Diagonal components and isotropic value of the polarizability as a function of the reaction coordinate for Br_2 addition to C_2H_2 in the gas phase

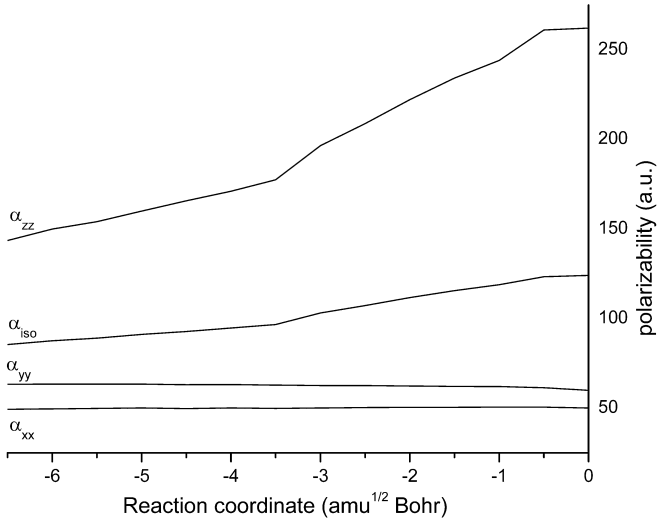

Fig. 12. Diagonal components and isotropic value of the polarizability as a function of the reaction coordinate for Br_2 addition to C_2H_2 in water

atoms are along the *z*-axis and the ethylene is on the *xy*-plane with the CC bond along the *y*-axis.

The analysis of the polarizability along the RP amplifies the differences previously found for the geometry and the natural charges on passing from the gas phase to water solution: for the gas phase we observe an increase of the *zz* component (and of the isotropic value) going from the TS back to the CTC, while for water both α_{zz} and α_{iso} monotonically decrease. As expected, in both cases the *xx* and *yy* components do not significantly vary along the RP.

The results obtained for water are in good agreement with theoretical evidence showing that in general the TS has a higher polarizability than the reactive complex [43]. Conversely, the gas-phase trend of the polarizability along the RP indicates that the reactive channel involves an unfavorable charge redistribution going from the CTC to the TS and thus it will be characterized by a high activation energy barrier. These findings strengthen the optimism about the possibility of using polarizability as an index for the study of the progress of chemical binding and reactions.

6 Conclusion

We have presented a methodology to evaluate MP2 second derivatives for solvated systems described within the PCM. The method is based on the differentiation of the response density equations for first derivatives; however, the need for the solution of additional CPHF-like (**Z**-vector) equations is avoided entirely by the use of an additional interchange theorem. This method is an extension to solvated systems of a formalism, and of the corresponding algorithm, originally developed for isolated systems and implemented as part of the Gaussian program suite. The main feature of this extension is that no approximations are introduced for the PCM additional contributions but they are included in any step of the procedure, i.e. in the CPHF-like equations as well as in the derivatives of the free energy.

The algorithm described herein was applied to the study of the rate-determining step of the electrophilic addition of bromine to ethylene in aqueous solution. Analytical MP2 first and second derivatives with respect to nuclear displacements allowed us to locate intermediates and TS structures, as well as to evaluate the projected vibrational frequencies, and analytical MP2 second derivatives with respect to electric fields were used to compute the polarizability tensor along the RP. In addition, the relaxed MP2 density was used in a NBO analysis of the charge character of the CTC and the TS as well as of structures along the RP.

The results about the nature of both the CTC and the TS not only are in substantial agreement with the data available from the literature, but they also permit a more detailed analysis of the fundamental role played by solvation in this kind of reaction. In particular, the analysis of the natural charges on the various atoms and of the polarizability tensors along the RP clearly indicates that the stabilizing effect due to the polar solvent is the necessary, and sufficient, effect required to make the reaction possible through the formation of a TS with well-separated charges on the bromine atoms; this system can thus easily evolve toward the bromonium cation, which is assumed as the key intermediate of the reaction.

As a final comment, we remark that both in the theoretical derivation and in the numerical application, a complete solvent response to molecular vibrations (equilibrium model) was assumed. However, it is also reasonable to think that the solvent molecules surrounding the solute could not instantaneously rearrange their position to re-equilibrate with respect to the vibrating solute (and thus that a vibrational non equilibrium model could be used). Such effects have already been treated for vibrational frequencies, IR intensities and Raman scattering activities for solutes modeled at

the HF and density functional theory levels of theory within the PCM framework [44]. The results reported in the references cited have shown that vibrational non-equilibrium effects seem to be relevant in the prediction of absorption intensities and Raman scattering activities, whereas they affect vibrational frequencies only negligibly. We are thus confident that the results we reported in the previous section, as mainly based on geometrical second derivatives, do not change in a nonequilibrium scheme. However, we are perfectly aware that in accurate dynamic studies, nonequilibrium, or more generally time-dependent solvation effects, are fundamental; we thus leave to future extensions inclusions of such effects into MP2 second derivatives.

Acknowledgements. R.C., B.M, C.P., C.C., S.C. and L.F. thank Professor Tomasi for having introduced them to the fascinating field of quantum chemistry. His careful and discreet advice together with his extraordinary chemical knowledge have cultivated the enthusiasm and the responsibility of each one while always preserving their different personal attitudes. Thanks to his example, research has become a unique adventure for each of them.

References

1. (a) Pulay P (1987) In: Lawley KP (ed) Advances in chemical physics, vol 49 Wiley, Chichester, 241; (b) Yamaguchi Y, Goddard JD, Schaefer HF III (1994) A new dimension to quantum chemistry: analytic derivative methods in ab initio molecular electronic structure theory. Oxford University Press, Oxford
2. Tomasi J, Persico M (1994) Chem Rev 94: 2027
3. Miertus S, Scrocco E, Tomasi J (1981) Chem Phys 55: 117
4. Cammi R, Tomasi J (1995) J Comput Chem 16: 1449
5. (a) Cancès E, Mennucci B (1998) J Math Chem 23: 309 (b) Cancès E, Mennucci B, Tomasi J (1997) J Chem Phys 107: 3032; (c) Mennucci B, Cancès E, Tomasi J (1997) J Phys Chem B 101: 10506
6. Tomasi J, Cammi R, Mennucci B, Cappelli C, Corni S (2002) Phys Chem Chem Phys 4: 5697
7. Cammi R, Tomasi J (1994) J Chem Phys 100: 7495; (b) Cammi R, Tomasi J (1994) J Chem Phys 101: 3888
8. (a) Cancès E, Mennucci B (1998) J Chem Phys 109: 249; (b) Cancès E, Mennucci B, Tomasi J (1998) J Chem Phys 109: 260
9. Mennucci B, Cammi R, Tomasi J (1999) J Chem Phys 110: 6858
10. Cossi M, Scalmani G, Rega N, Barone V (2003) J Chem Phys 117: 43
11. Cammi R, Mennucci B, Tomasi J (2000) J Phys Chem A 104: 5631
12. Cammi R, Mennucci B, Tomasi J (1999) J Phys Chem A 103: 9100
13. (a) Olivares del Valle FJ, Tomasi J (1991) Chem Phys 150: 139; (b) Aguilar MA, Olivares del Valle FJ, Tomasi J (1991) Chem Phys 150: 151; (c) Olivares del Valle FJ, Aguilar MA (1993) J Mol Struct (THEOCHEM) 280: 25; (d) Olivares del Valle FJ, Aguilar MA, Tolosa S (1993) J Mol Struct (THEOCHEM) 279: 223
14. Ángyán JG (1993) Int J Quantum Chem 47: 469
15. Handy NC, Schaefer HF III (1984) J Chem Phys 81: 5031
16. Frisch MJ et al (2000) Gaussian development version Gaussian Pittsburgh, PA
17. Head-Gordon M, Head-Gordon T (1994) Chem Phys Lett 220: 122
18. Salter EA, Trucks GW, Fitzgerald G, Bartlett RJ (1987) Chem Phys Lett 141: 61
19. (a) Pople JA, Krishnam HB, Schlegel B, Binkley JS (1979) Int J Quantum Chem 13: 225; (b) Gaw JF, Handy NC (1984) Annu Rep R Soc Chem C 291; (c) Gauss J, Cremer D (1992) Adv Quantum Chem 23: 205
20. (a) Frisch MJ, Head-Gordon M, Pople J (1990) Chem Phys Lett 166: 275; (b) Frisch MJ, Head-Gordon M, Pople J (1990) Chem Phys Lett 166: 281
21. (a) Fukui K (1981) Acc Chem Res 14: 363; (b) Page M, McIver JW Jr (1988) J Chem Phys 88:922; (c) Ishida K, Morokuma K, Komornicki A (1977) J Chem Phys 66: 2153; (d) Schmidt MW, Gordon MS, Dupuis M (1985) J Am Chem Soc 107: 2585; (e) Garrett BC, Redman MJ, Steckler R, Truhlar DG, Baldridge KK, Bartol D, Schmidt MW, Gordon MS (1988) J Phys Chem 92: 1476; (f) Baldridge KK, Gordon MS, Steckler R, Truhlar DG (1989) J Phys Chem 93: 5107
22. (a) Gonzales C, Schlegel HB (1989) J Chem Phys 90: 2154; (b) Baboul AG, Schlegel HB (1997) J Chem Phys 107: 9413
23. Miller WH, Handy NC, Adams JE (1980) J Chem Phys 72: 99
24. (a) Garrett BC, Truhlar DG (1979) J Chem Phys 70: 1593;(b) Truhlar DG, Garrett BC (1984) Annu Rev Phys Chem 35: 159
25. (a) Bianco R, Miertus S, Persico M, Tomasi J (1992) Chem Phys 168: 281; (b) Aguilar M, Bianco R, Miertus S, Persico M, Tomasi J (1993) Chem Phys 174: 397;(c) Tomasi J (1994) ACS Symp Ser 568: 10; (d) Coitino EL, Tomasi J, Ventura ON (1994) J Chem Soc Faraday Trans 90(12): 1745
26. Tomasi J, Mennucci B, Cammi R, Cossi M, (1997) In: Naray-Szabo G, Warshel A (eds) Computational approaches to biochemical reactivity. Kluwer, Dordrecht, p 1, and references therein
27. Freeman F (1975) Chem Rev 75: 439
28. Jaszunski M, Kochanski E (1977) J Am Chem Soc 99: 4624
29. Toyonaga B, Peterson MR, Schmid GH, Csizmadia IG (1983) J Mol Struct (THEOCHEM) 11: 363
30. Ruiz E, Salahub DR, Vela A (1995) J Am Chem Soc 117: 1141
31. Bloemink HJ, Hinds K, Legon AC, Thorn JC (1994) J Chem Soc Chem Commun 1321
32. Smirnov VV, Tikhomirov VA, Chudinov GE (1993) J Struct Chem 34: 501
33. Angelini G, Speranza M (1981) J Am Chem Soc 103: 3792
34. Yamabe S, Minato T, Inagaki S (1988) J Chem Soc Chem Commun 532
35. Ruasse MF, Motallebi S, Galland B (1991) J Am Chem Soc 113: 3440
36. Cossi M, Persico M, Tomasi J (1994) J Am Chem Soc 116: 5373
37. Assfeld X, Garapon J, Rinaldi D, Ruiz-Lopez MF, Rivail JL (1996) J Mol Struct (THEOCHEM) 371: 107
38. (a) Stevens W, Basch H, Krauss J (1984) J Chem Phys 81: 6026; (b) Stevens W, Krauss J, Basch H, Jasien PG (1992) Can J Chem 70: 612
39. Amovilli C, Floris FM, Mennucci B (1999) Int J Quantum Chem 74: 59
40. Bienvenue-Goetz E, Dubois JE (1968) Tetrahedron 24: 6777
41. Glendening ED, Reed AE, Carpenter JE, Weinhold F, NBO version 3.1
42. (a) Politzer P (1987) J Chem Phys 86: 1072; (b) Ghanty T K, Ghosh SK (1993) J Phys Chem 97: 4951; (c) Roy R, Chandra AK, Pal S (1994) J Phys Chem 98: 10447; (d) Simon-Manso Y, Fuenteaelba P (1998) J Phys Chem A 102: 2029
43. (a) Ghanty TK, Ghosh SK (1996) J Phys Chem 100: 12295; (b) Safi B, Choho K, Geerlings P (2001) J Phys Chem A 105: 591
44. (a) Cappelli C, Corni S, Cammi R, Mennucci B, Tomasi J (2000) J Chem Phys 113: 11270; (b) Cappelli C, Corni S, Tomasi J (2001) J Chem Phys 115: 5531.